Theor Chem Acc (2005) 114: 153–158
DOI 10.1007/s00214-005-0656-x

REGULAR ARTICLE

M. Makowska-Janusik · H. Reis
M. G. Papadopoulos · I.G. Economou

Peculiarities of electric field alignment of nonlinear optical chromophores incorporated into thin film polymer matrix

Received: 2 August 2004 / Accepted: 3 September 2004 / Published online: 30 May 2005

Abstract The electric field poling process of free-standing films of poly(methyl methacrylate) (PMMA) matrix doped with the nonlinear optical compound 4-(dimethylamino)-4'-nitrostilbene (DMANS) was investigated by molecular simulation methods. The influence of the vacuum/bulk interfacial regions on static and dynamic properties, including the glass transition temperature T_g and the field-induced chromophore reorientation, was studied by employing films of three different thicknesses and by comparison with previous work on the bulk system. The interfacial region, defined as the region, where the local density increases from zero to the bulk density, is about 2 nm wide, independent of the film thickness. T_g decreases with decreasing film thickness, in accord with previous experimental work and theoretical predictions. The resistance against field-induced chromophore reorientation in the liquid state is found to increase strongly with the film thickness.

1 Introduction

Over the past few years polymeric films have received considerable attention, because they appear to exhibit thermodynamic, structural and dynamic properties different from those of the bulk material [1, 2]. A large surface area to volume ratio characterizes a thin film. The surface properties of polymers are potentially a critical factor in determining performance and suitability in films and coatings [3]. Numerical methods can help to understand questions connected with surface mobility, glass transition behavior and the conformational properties of thin polymeric films.

A process for the fabrication of a second-order nonlinear optical (NLO) polymer is electric field poling. A typical glassy polymer containing chromophores that have large second-order susceptibility is heated and poled near the glass transition temperature (T_g) to create a non-centrosymmetric structure, then cooled below the T_g while still applying the electric field. After the external field is removed, a net alignment of dipole moments remains essentially locked in the film. The poled films resulting from this procedure usually have limited lifetimes due to structural relaxation, for the case of conventional polymers [4a]. In recent years, considerable progress has been made toward the development of novel highly efficient NLO dendrimers and cross-linkable polymers that provide optimum electro-optic activity, thermal stability and optical loss. In this way, nanoscale architectural control results in materials that are significantly better than conventional NLO materials [4b].

Recent studies on various low-dimensional materials have demonstrated that most of the structural, mechanical, optical and electronic properties are thickness-dependent [5]. The goal of this work was the investigation of the influence of varying interface/bulk ratios on static and dynamic properties of an electric field poled host–guest system. Fully atomistic simulations were performed on the electric field poled PMMA/DMANS system. The approach applied in this work is similar to the previous work on bulk host-guest systems, including PMMA/DMANS [6]. The motivation for the present work was the question if the surface influences the chromophores reorientation dynamics investigated in the bulk in Ref. [6].

The molecular model and methods of the simulations are presented in the following section. The consequences of the molecular dynamic (MD) simulations and discussion of the results are described under Results and Discussion, followed by a short Summary.

M. Makowska-Janusik (✉)
Institute of Physics, WSP, Al. Armii Krajowej 13/ 15, PL-42201 Czestochowa, Poland
e-mail: m.makowska@wsp.czest.pl

H. Reis · M. G. Papadopoulos
Institute of Organic and Pharmaceutical Chemistry, National Hellenic Research Foundation, Vasileos Constantinou 48, GR-11635 Athens, Greece
e-mail: hreis@eie.gr, mpapad@eie.gr

I.G. Economou
Molecular Modeling of Materials Laboratory, Institute of Physical Chemistry, National Research Center for Physical Sciences "Demokritos", GR 15310 Aghia Paraskevi Attikis, Greece
e-mail: economou@mistras.chem.demokritos.gr

2 Simulation model

Three thin films of different thickness were constructed. The unit cell of the first film, called film I in the following, was a cube with edge length 2.511 nm, containing one isotactic PMMA 90-mer (with molecular weight equal to 9012.58 amu) and two DMANS molecules (5.6 wt %). For the second (film II) and third (film III) films the length of the unit cell in the direction perpendicular to the film was doubled and tripled, respectively, leading to a unit cell of dimensions of $2.511 \times 2.511 \times 5.022$ nm containing two PMMA 90-mer chains and four DMANS molecules for film II and $2.511 \times 2.511 \times 7.533$ nm for film III, with three PMMA 90-mers and six DMANS molecules. The starting structures for these thicker films were produced by double and triple replication, respectively, of the content of the unit cell of the film I. The film thicknesses of film I, film II and film III are approximately equal to 2, 4 and 6 radii of gyration (R_g), respectively, of the PMMA chain. Using the simulation results of Ref. [6], R_g has been calculated to be equal to 1.21 nm. This quantity has been calculated using the formula

$$R_g = \left\langle \left(\sum_{i=1}^{N} m_i (r_i - r_c)^2 / \sum_{i=1}^{N} m_i \right)^{1/2} \right\rangle , \qquad (1)$$

where r_c are the coordinates of the center of mass, and $<\ldots>$ denotes ensemble averaging.

The density for all systems was 1.00 g/cm^3, corresponding to the liquid state system. For each film three different structures were simulated. The initial configuration of the smallest cell was generated using Amorphous Cell, a module of the Cerius2 software package [8], while the replication of the cubic cell, as well as all molecular simulations, were done using the GROMACS software package [9]. Each configuration was minimized by conjugate gradient method employing a convergence criterion of 10 kcal mol^{-1}Å^{-1}, followed by a NVT MD simulation. The MD was carried out for 1 ns at 500 K using a step size of 1 fs. Thereafter, the three lowest energy configurations of these runs were again minimized by conjugate gradient methods, this time applying a convergence criterion of 0.1 kcal mol^{-1}Å^{-1} . The all-atom consistent valence force field (CVFF) [10–12] was selected for the present MD study. The CVFF has been used previously to represent the potential energy surface of the PMMA polymer [13]. The force field parameters for the considered molecules and parameters of the MD simulation are given in [6]. Following the energy minimization and prior to the production cycle of MD, all the considered structures were relaxed for 2 ns of real time in order to obtain the equilibrium state of the systems. The total energy of the simulated systems was constant for all structures after about 1 ns relaxed process.

Then, all structures were simulated at temperature $T = 500$ K, which is above the glass transition temperature T_g, using two-dimensional (2D) periodic boundary conditions. The long-range non-bonded interactions were calculated using the 2D particlemesh Ewald method (PME) [14] in order to simulate thin films with infinite extensions along X and Y-axis and finite length in Z-direction. The trajectories were recorded every picosecond. The simulations were performed in the NVT canonical ensemble using the Nose–Hoover extended ensemble [15,16] to keep the temperature constant. After this unpoled, liquid state simulation which were running during 1.5 ns, a poling external electric field was applied in Z-direction and the structures were simulated for a further 1.5 ns. The ability of the films to reach a stationary state with respect to the poling field in the time window of the simulation was investigated by applying different field strengths. In the next simulation step the films were solidified in the presence of the poling electric fields using the simulated annealing method described in detail in Ref. [6]. The samples were cooled from 500 K up to 300 K during 1.5 ns with a cooling rate of 1.3×10^{11} K/s. The final density for all films was 1.173 ± 0.005 g/cm^3, corresponding to the experimental value of the glassy state of PMMA [7].

The poled, sub-T_g systems were simulated at constant NVT conditions, with poling field applied, for a further 1.5 ns, which were used to analyze the poled, high-density systems. Finally, to investigate the system stability and back-relaxation of the chromophores, the poling field was removed, and 1.5 ns MD simulations under NVT conditions were performed.

The glass transition temperature T_g was determined from density–temperature plots as described in Ref. [6]. The systems were simulated under NPT conditions employing the Rahman–Parrinello pressure coupling [17] and the Nosé–Hoover thermostat [15,16]. We used this barostat/thermostat combination because it allows to probe the exact NPT ensemble, contrary to the second coupling scheme available in GROMACS, that is Berendsen coupling. Additionally, experiments conducted during the work for Ref. [6] showed that with Berendsen pressure coupling the pressure oscillations in the equilibrated state simulations were generally larger than with Rahman–Parrinello coupling. In order to keep the films from disintegrating during the NPT simulations, a large pressure (1000 atm) was applied perpendicular to the film surface. This high pressure led to a considerable density compression of the films during the simulated annealing compared to the corresponding bulk simulations of Ref. [6].

3 Results and discussion

The dependence of the density on the temperature for the three films of varying thickness is shown in Fig. 1. From these plots the following glass transition temperatures T_g were deduced, using linear regression analysis as applied in Ref. [6]: (420 ± 30) K for film III, (390 ± 30) K for film II and (320 ± 30) K for the thinnest film I. The simulated T_g value for the bulk PMMA/DMANS system was (450 ± 50) K [6]. In spite of the large error margins these values indicate clearly a decrease of T_g in going from the bulk to the film and with decreasing film thickness. Such a thickness dependent T_g value for thin films is in accord with experimental [18] as well as theoretical [19,20] works. It is argued that the excess free volume near the surface is larger than deep in the bulk,

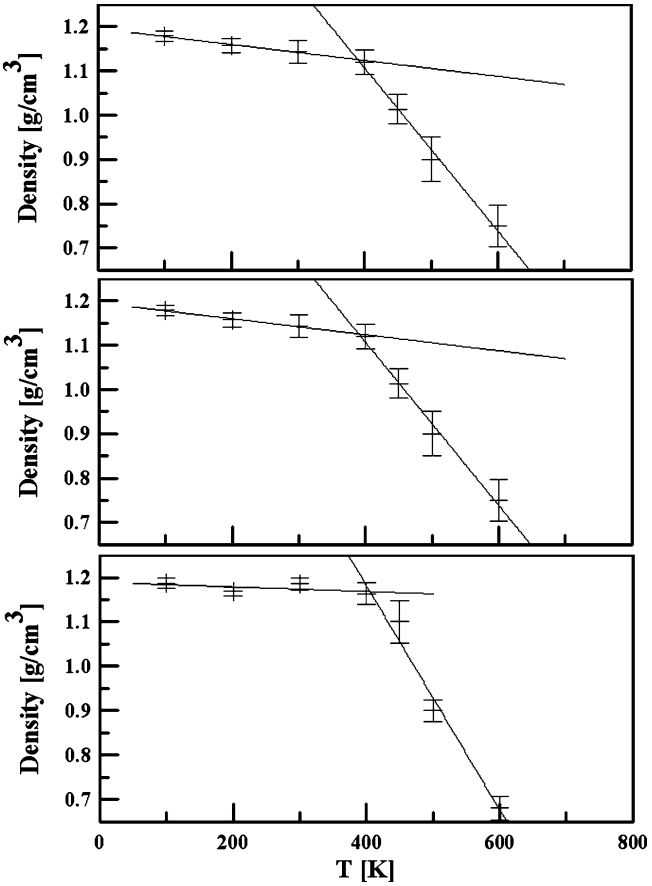

Fig. 1 Glass transition temperature predicted by MD simulations for the PMMA/DMANS systems with different thickness. Note the difference in the density scale for film I

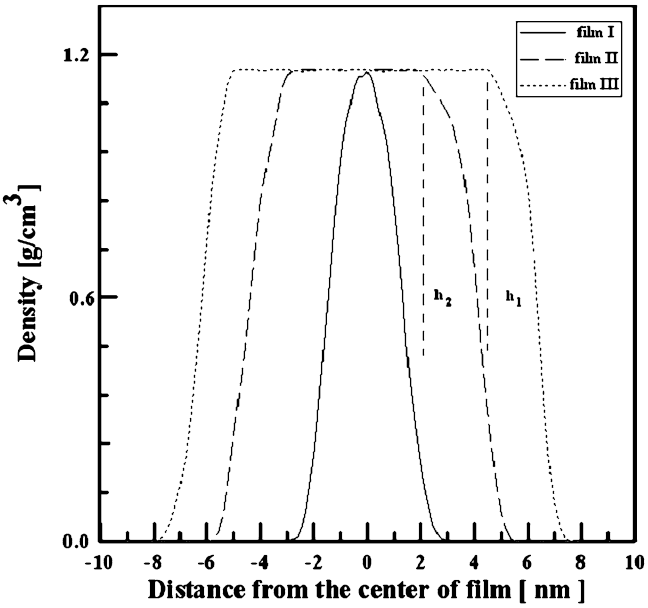

Fig. 2 Density profiles of the PMMA/DMANS films of the different thickness at $T = 300$ K versus the distance from the center of film

leading to a higher mobility of polymer chain segments near the surface, which decreases T_g with increasing surface to bulk ratio [21–23]. Other effects influencing T_g are the nature of the substrate of coated films [24,25] and the molecular weight of the polymer [26], both of which could not be explored here. We note that direct comparison of the simulated T_g values with experimental ones is not possible due to the unrealistically high cooling rates applied in the simulations (up to 1.3×10^{11} K/s), which generally lead to T_g values that are too high compared with the experiment [27].

The density profiles for the three considered films at $T = 300$ K are shown in Fig. 2. The densities were calculated by counting the nuclei as a function of the distance from the center of mass of the film and then averaged over all configurations in the simulation. The density profiles were obtained by fitting to a hyperbolic function of the distance, as introduced by Helfand and Tagami [28]. The density profiles of film II and film III show a region of nearly constant maximum density of (1.16 ± 0.05) g/cm^3, which is well separated from the interfacial regions. The density profile of film I, on the other hand shows no such region of constant density; the two interfacial regions, where the density is strongly distance-dependent, are nearly directly connected. This is in agreement with simulation work of Jang and coworkers on polyethylene melts [29]. The density for the bulk PMMA/DMANS system simulated at $T = 300$ K was 1.20 g/cm^3 [6]. This result, based on density considerations only, indicates that the film should be at least as thick as film II in order to produce a bulk internal structure with a constant density. As shown by the arrows in Fig. 2 the thickness of the interfaces for the two thicker films are very similar for the two films and equal to 2 nm. We conclude that the interface layer is an intrinsic polymer property and does not depend on the film thickness.

As the rotational flexibility of the dopant depends on the conformational mobility of polymer, we investigated the conformational properties of PMMA for the simulated films. First, the population distributions of the two dihedral angles of the polymer were computed and were found to be similar among the films and to corresponding distributions of the bulk system [6]. They show symmetric distributions for both angles with three highly populated states: near trans, gauche+ and gauche−. This confirms our results [6] and that of Kim and Hayden [30], that the distribution of the torsion angles of the PMMA and its flexibility is an intrinsic property of the polymer and is not affected by the dopant and the poling process.

The mobility of the polymer in the films has been characterized by the torsional autocorrelation function (TACF) [31]. As has been found for the bulk PMMA/DMANS system [6], the rotational mobility of the side groups of PMMA is higher than that of the backbone, therefore the surface does not affect the different flexibilities of backbone and side groups of the polymer. As found for the bulk, the external electric field affects the flexibility of PMMA segments. For all three films the external electric filed decreased the mobility of the investigated groups of polymer, both in the liquid and in the glassy state.

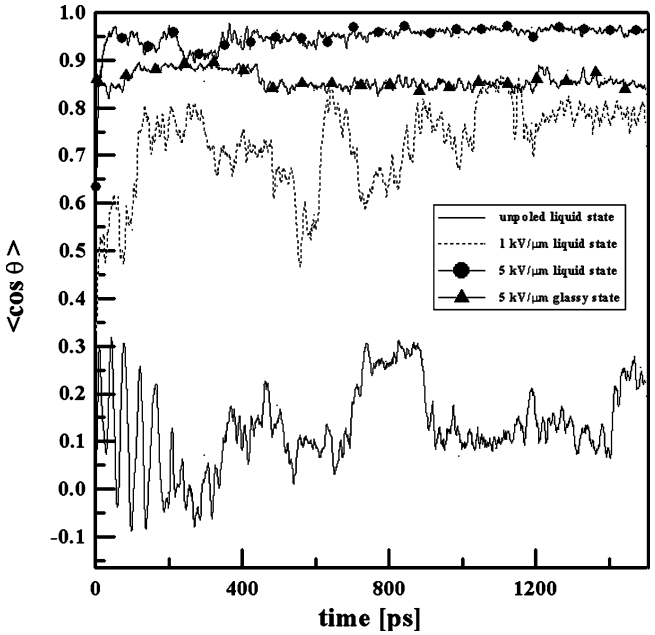

Fig. 3 The average value of the dipole moment vector of DMANS, along the field direction, for electric field poled and unpoled structures for film I

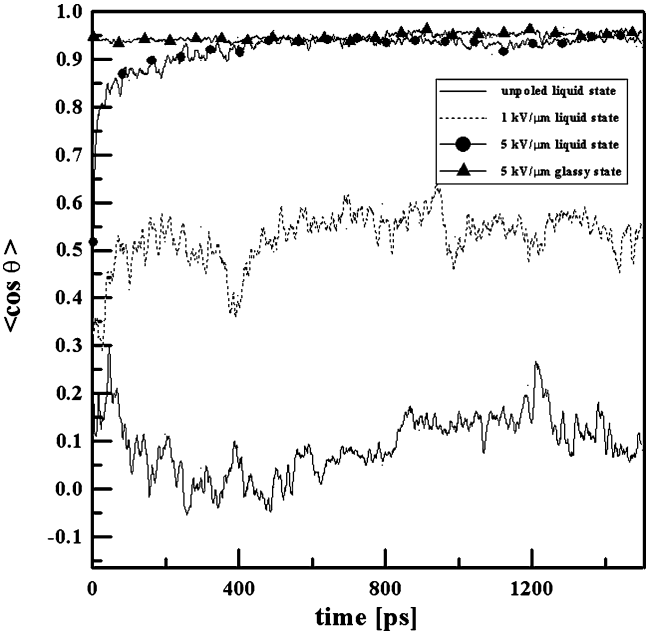

Fig. 4 The average value of the dipole moment vector of DMANS, along the field direction, for electric field poled and unpoled structures for film II

In order to investigate the field induced alignment of the dopants we computed the parameters $\langle\cos\theta\rangle$ and $\langle\cos^3\theta\rangle$, where θ is the angle between the dopants' dipole moment and the poling field and the brackets denote ensemble averaging. By comparing the simulated values with those of the Langevin functions $L_1(p)$ and $L_3(p)$ [32], corresponding to a Boltzmann distribution, it is possible to assess how far the simulated systems have reached the stationary state with respect to the poling field. In the stationary state the following equations hold:

$$\langle\cos\ \theta\rangle = \coth p - \frac{1}{p} = L_1(p) \tag{2}$$

$$\langle\cos\ ^3\theta\rangle = \left(1 + \frac{6}{p^2}\right) L_1(p) - \frac{2}{p} = L_3(p)\,, \tag{3}$$

where $p = \underline{\mu} \cdot \underline{E} \Big/ kT$.

The time-dependent properties $\cos\theta(t)$ before and during poling with different field strengths and in the glassy state are shown in Figs. 3–5. In Table 1 the computed ensemble averaged parameters are compared with the Langevin functions obtained from Eqs. (2) and (3).

One can see that in the liquid, unpoled state of the chromophores are approximately randomly oriented; $\cos\ \theta(t)$ fluctuates around zero. The fluctuations of $\cos\ \theta(t)$ in film I are larger than those obtained for the thicker films. This may be explained by the absence of a proper "bulk" region in this film, as shown above, which means that the chromophores are mostly in regions of reduced density and therefore more mobile.

The data in Table 1 show a pronounced dependence of the necessary poling field strength to achieve or at least approximate the stationary state in the time scale used for our simulations on the film thickness: film I subjected to a field strength of 5 kV/μm reaches the stationary state as characterized by the Langevin function values in 1.5 ns poling time, while with a field of 1 kV/μm one obtains a fairly well approximation to the stationary state value; for film II, 5 kV/μm leads to an acceptable approximation, while film III requires al-

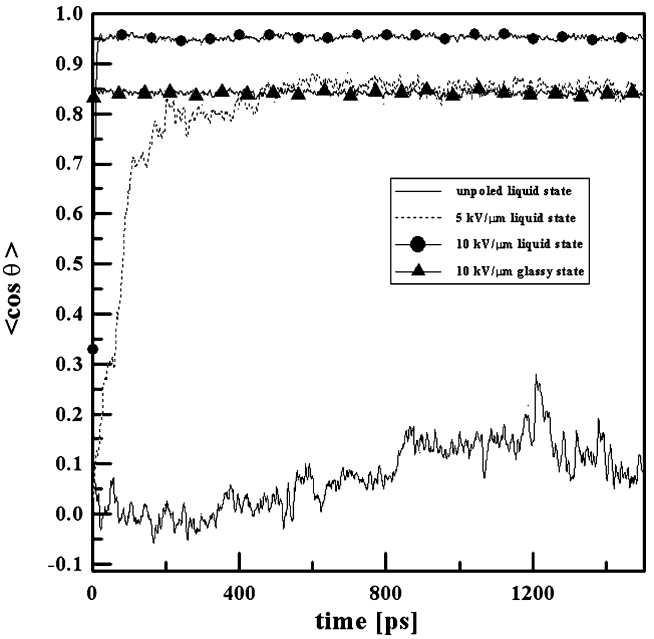

Fig. 5 The average value of the dipole moment vector of DMANS, along the field direction, for electric field poled and unpoled structures for film III

Table 1 The order parameters $\langle \cos\ \theta \rangle$ and $\langle \cos\ ^3\theta \rangle$ calculated from MD simulations and the theoretically predicted values $L_1(p)$ and $L_3(p)$ (Liquid state: $T = 500$ K, glassy state: $T = 300$ K)

Film	I			II			III		
Order parameters	Liquid state		Glassy state	Liquid state		Glassy state	Liquid state		Glassy state
	1 kV/μm	5 kV/μm	1 kV/μm	1 kV/μm	5 kV/μm	5 kV/μm	5 kV/μm	10 kV/μm	10 kV/μm
$L_1(p)$	0.79	0.96	0.88	0.79	0.96	0.97	0.96	0.98	0.99
$L_3(p)$	0.58	0.89	0.71	0.58	0.89	0.93	0.89	0.94	0.95
$\langle \cos\ \theta \rangle$	0.72 ± 0.22	0.96 ± 0.04	0.86 ± 0.10	0.52 ± 0.23	0.94 ± 0.06	0.94 ± 0.05	0.85 ± 0.18	0.95 ± 0.04	0.90 ± 0.10
$\langle \cos\ ^3\theta \rangle$	0.47 ± 0.29	0.89 ± 0.10	0.66 ± 0.21	0.21 ± 0.15	0.81 ± 0.17	0.88 ± 0.08	0.69 ± 0.23	0.88 ± 0.11	0.75 ± 0.24

ready a 10 kV/μm poling field strength to arrive at an approximately stationary state. For the bulk system, field strength of 15 kV/μm had to be used to achieve a similar approximation to the stationary state [6]. The main explanation for this thickness effect can probably be found again in the different ratios of interface regions of low local density, where chromophore reorientation is easy, to bulk volume of high density, with increased resistance against reorientations, for the different films.

Comparison of the order parameters given in Table 1 for the glassy state and for the liquid state shows that the behavior during the simulated cooling under influence of the poling field is thickness-dependent, too: for film I the order parameters *increase* during the cooling process, for film II they stay approximately constant, while for film III they *decrease*. This last behavior is again in accord with that found for the bulk system [6], and was explained by the very fast time scale of the cooling process, which does not allow for the additional relaxation necessary to reach the stationary state in the high-density system. This is probably no problem for film I where the lower local density around the chromophores allows for additional reorientation, while for film II the two effects just balance each other.

The back-relaxation of the aligned chromophores in the glassy state was also investigated. The $\cos\ \theta(t)$ values were calculated at $T = 300$ K after switching off the poling external electric field. As for the bulk system, the functions were fitted to a bi-exponential function $\cos\ \theta(t) = A \exp\left(-t/\tau_1\right) + B \exp\left(-t/\tau_2\right)$. While one of the relaxation times is in the region of ms to s, and therefore not accessible at all by our simulations of 1.5 ns duration, the "fast" relaxation time is in the range of 10–100 ps and has been tentatively connected with reorientation in residual free volume [6]. For film I, we find a fast relaxation time of 40 ps, while in the bulk it was 62 ps [6]. This difference may again be explained by lower local density around the chromophores in film I, leading on the one hand to a faster alignment in the poling field in the liquid, which does not need to be so large as that for the bulk, but on the other hand also leads to a faster randomization of the dipole moment vector distribution in the glassy state.

4 Summary

The process of electric-field poling of thin films of varying thickness of the NLO guest–host system DMANS/PMMA have been investigated by molecular dynamics. The glass transition temperature as well as the necessary poling field strength to achieve a stationary state in the time window of the molecular simulation has been found to be strongly thickness dependent. Both effects can be explained by the differing ratios of the volume of interfacial region with reduced local density to the volume of the bulk region where the density is high and approximately constant. Although the lower field strengths necessary for chromophore alignment in thinner films may be considered an advantage in real applications, it appears also to be connected with a faster back-relaxation in the glassy state after removal of the field, which would be definitely a disadvantage in applications. One should note, however, that we only investigated *very thin, freely standing* films. Real films are generally spread on substrates, which introduce new features, and are usually thicker than those simulated here. Finally, molecular simulation studies can be further extended to the more complex recently developed dendritic EO materials [4b].

Acknowledgements MGP acknowledges a Marie Curie Host Development Fellowship (HPMD-CT-2001-00091). MMJ who was the Marie Curie Fellow, is grateful for her grant.

References

1. Clancy TC, Mattice WL (1999) Comp Theoret Polym Science 9:261
2. Ral J (1999) Current Option Colloid Interface Sci 4:153
3. Ayyagari Ch, Bedrov D, Smith GD (2004) Polymer 45:4549
4. (a) Hampsch HL, Yang J, Wong GK, Torkelson JM (1988) Macromolecules 21:526; (b) Luo J, Haller M, Ma H, Liu S, Kim T-D, Tian Y, Chen B, Jang S-H, Dalton LR, Jen AK-Y (2004) J Phys Chem B 108:8523
5. Bruggemann R, Reinig P, Holling M (2003) Thin solid films 427:358; Zhou H, Shi FG, Zhao B (2003) Microelectronics J 34:259
6. Makowska-Janusik M, Reis H, Papadopoulos MG, Economou IG, Zacharopoulos N (2004) J Phys Chem B 108:588–596
7. Sane SB, Cagin T, Goddard WA, Knauss WG (2002) J Comput Aided Mater 8:87
8. www.accelrys.com/cerius2/
9. Berendsen HJC, van der Spoel D, van Drunen R (1995) Comput Phys Commun 91:43; Lindahl E, Hess B, van der Spoel D (2001) J Mol Modell 7:306; van der Spoel D, van Buuren AR, Apol E, Tieleman PJ, Sijbers ALM, Hess B, Feenstra KA, Lindahl E, van Drunen R, Berendsen HJC (2002) GROMACS user manual; Department of Biophysical Chemistry, University of Groningen: Groningen, Netherlands
10. Hagler AT, Huler E, Lifton S (1974) J Am Chem Soc 96:5319
11. Kitson DH, Hagler AT (1988) Biochemistry 27:5246

12. Dauber-Osguthorpe P, Roberts VA, Osguthorpe DJ, Wolff J, Genest M, Hagler AT (1988) Proteins: Struct Funct Genet 4:31
13. Young JA, Farmer BL, Hinkley JA (1999) Polymer 40:2787
14. In-Chul Y, Berkowitz ML (1999) J Chem Phys 111:3155
15. Nose S (1984) Mol Phys 52:255
16. Hoover GW (1985) Phys Rev A 31:1695
17. Parrinello M, Rahman A (1981) J Appl Phys 52:7182
18. Fryer DS, Nealey PF, de Pablo JJ (2000) Macromolecules 33:6439; Singh L, Ludovice PJ, Henderson CL (2004) Thin Solid Films 449:231; Forrest JA, Dalnoki-Veress K (2001) Advances in Colloid and Interface Science 94:167
19. Torres JA, de Pablo JJ (2000) Phys Rev Lett 85:3221
20. Jain TS, De Pablo JJ (2002) Macromolecules 25:2167
21. Mayes AM (1994) Macromolecules 27:3114
22. Kajiyama T, Tanaka K, Takahara A (1997) Macromolecules 30:280
23. Pham JQ, Green PF (2002) J Chem Phys 116:5801
24. Zhou H, Kim HK, Shi FG, Zhao B, Yota J (2002) Microelectronics J 33:221
25. Keddie JL, Ral J, Cory RA (1995) Faraday discuss 98:219
26. Ferry DJ (1980) Viscoelastic properties of polymers 3rd ed Wiley, New York
27. Hedenqvist MS, Bharadway R, Boyd RH (1998) Macromolecules 31:1556
28. Helfand E, Tagami Y (1972) J Chem Phys 57:1812
29. Jang JH, Ozisik R, Mattice WL (2000) Macromolecules 33:7663
30. Kim W-K, Hayden LM (1999) J Chem Phys 111:5212
31. van der Spoel D, Berendsen HJC (1997) Biophys J 72:2002
32. Williams DJ (1987) Nonlinear optical properties of guest–host polymer structures. In: Chemla DS, Zyss J (eds) Nonlinear optical properties of organic molecules and crystals. Academic, New York